ARTICLE TEMPLATE

Unknown Input Observer for Quadratically Inner Bounded-One Sided Lipschitz Perturbed Nonlinear Systems

Juan Pablo Arango[a,b], Lucien Etienne[a], Eric Duviella [a], Kokou Langueh [a] Pablo Segovia [b,c] Vicenç Puig [b,c]

[a]IMT Nord Europe-SERI SN, Douai, France; [b]Department of Automatic Control, Universitat Politècnica de Catalunya, Barcelona, Spain; [c] Institut de Robòtica i Informàtica Industrial, CSIC-UPC, Barcelona, Spain

ARTICLE HISTORY
Compiled February 10, 2025

ABSTRACT
In this paper, the problem of designing an observer for quadratically inner bounded (QIB) and one-sided Lipschitz (OSL) nonlinear systems considering perturbations in the output and unknown inputs is addressed. The observer synthesis procedures are formulated as convex optimization problems. Sufficient conditions for observer gain synthesis are shown to be equivalent to solve finite sets of Linear Matrix Inequalities (LMIs) and Linear Matrix Equalities (LMEs). Three illustrative examples based on an isothermal CSTR reactor, a water tank-open channel system and FitzHugh-Nagumo system are used to illustrate how the proposed approaches are used to design the QIB-UIO scheme. The obtained simulation results are presented to assess the performance of the proposed method.

KEYWORDS
One Sided Lipschitz , Quadratically Inner Bounded , Nonlinear systems , Unknown Input Observer , Observer design

1. Introduction

The supervision, control and predictive maintenance of a system generally requires the knowledge of its states. However, economic and technical constraints require the reduction of the number of physical sensors [1]. Moreover, the evolution of the system can be influenced by unmeasured perturbations, usually modelled as unknown inputs [2]. Thus, in the literature there are several studies focusing on reconstructing the state of a system from known inputs and outputs in the presence of unknown inputs. Such a task involves the synthesis of an Unknown Input Observer (UIO). Several contributions towards the design of UIO for linear systems can be found in the literature (see [3], [4]). However, the design of UIO for nonlinear systems (NLS) might become more challenging, as the validity of linear systems can only approximate the dynamic behavior of nonlinear systems in an interval around the operating point.

Nonlinear Lipschitz systems are a particular class of NLS, for which there are several results related to the design of UIO, see as e.g. in [5], [6]. The UIO synthesis problem for nonlinear Lipschitz systems is formulated in the Linear Matrix Inequalitiy (LMI) framework, obtaining sufficient conditions to guarantee the convergence of the error dynamics. Another family of systems, which is less restrictive than the Lipschitz one, is the family of Quadratically Inner Bounded (QIB) One-sided Lipschitz Nonlinear Systems (OSL). This type of systems has attracted the attention of the scientific community due to the fact that the bounding condition of the derivative must only be satisfied in the growth rate, but not in the decay rate, making it less restrictive than Lipschitz systems, which must satisfy both. Additionally, since the QIB condition is equivalent to Lipschitz [7], it adapts to the OSL condition by selecting sufficiently large QIB constants while also admitting negative constants, which is not possible when one wishes to describe a nonlinear system considering only the Lipschitz constant [8]. When designing control and estimation algorithms, the OSL-QIB property is preferred, since there is a greater number of parameters to describe the dynamics of a system, facilitating the convergence of these (compared with the Lipschitz one)[9]. In the present article, it is shown that the OSL-QIB description allows to find feasibility conditions for the formulated LMI, which is not possible to achieve considering the design of an observer with the classical Lipschitz constant [10], as is shown later in the paper by means of the FitzHugh-Nagumo (FHN) system example.

Some examples of UIO design for OSL-QIB systems can be found in the literature. For instance, the authors of [11] design a UIO robust against time delays. References [8], [12] and [13] present the design of UIO for OSL-QIB systems, OSL-QIB fractional NLS and OSL-QIB Markovian jump NLS, respectively. The previously cited authors succeed in proving that the UIO design conditions are reduced to satisfying certain LMI (convex optimization) constraints, as is the case for observer design including conventional Lipschitz conditions. Although previous works have considered the design of UIOs for OSL systems with different characteristics (e.g., time-delay and Markovian jump systems), the case in which perturbations are present in the measurement has not been considered yet. It is worth noting that this kind of perturbations are usually considered as noise in the literature [14–18]. Including this design condition is key because perturbations in the sensors (sensor uncertainty or noise) are always present when UIOs are implemented in real systems. Therefore, it is important to minimize the effect of perturbations in order to reduce the bias these can generate.

In this paper, a UIO is designed using an LMI approach for OSL-QIB systems. From a methodological point of view, the main contribution consists in the reformulation of the UIO synthesis problem for OSL-QIB systems as a convex optimization problem, while making the observer robust against sensor perturbations. This fact allows to solve the UIO synthesis problem for OSL-QIB systems and formulate the observer synthesis problem as a convex optimization problem by combining matrix inequalities and equalities. Using this approach, it becomes clear that sufficient conditions for UIO synthesis are identical to the ones considered for classical observer synthesis using LMIs (as considered for instance in [19]) combined with decoupling conditions between the observer error and the unknown input.

Summarizing the above, the main contributions of the paper are:

- To the best knowledge of the authors, the case with simultaneous noise and unknown inputs is considered for the first time.
- The design of observers that are robust against noise exists in several publications. However, the approximation considered therein is when the noise affects the state and then is propagated to the sensor (which does not always happen). In contrast, in this paper we consider the case the uncertainty is directly associated to the sensor, which in our opinion appears to be closer to reality.
- In the proposed approaches, the dynamical systems are written in terms of the

linearization error, which allows to write any dynamic system into a linear part, which depends on the observer gains, and the nonlinear part, which is bounded by the OSL-QIB constants.
- Application examples are provided to illustrate the interest and performance of the proposed approaches using the OSL-QIB system formulation.

The structure of the paper is the following: in Section 2, the problem statement is presented. Section 3 describes the UIO design procedures without and with noise. Section 4 shows the obtained results applying the proposed approaches using illustrative examples. Finally, Section 5 draws the main conclusions and points several future research paths.
Notations: $\mathbb{R}^n$ denotes the Euclidean space of dimension n, $\mathbb{R}^{n\times m}$ is the set of all $n \times m$ matrices. Matrices $P \prec 0$ and $P \succ 0$ are squared and symmetric, and negative and positive definite, respectively. The operation $\langle x, y\rangle = x^T y$ corresponds to the inner product between x and y, and x^T corresponds to the transpose of vector x. The operator $\mathcal{H}(A) = A + A^T$ is the Hermitian of A. Finally, $\|x\|$ is the norm of vector x.

2. Problem set-up

Consider the following nonlinear dynamical system:

$$\begin{aligned} \dot{x} &= Ax(t) + Bu(t) + D_f f(Hx) + Dv(t), \\ y &= Cx(t) + Rh(t), \end{aligned} \tag{1}$$

where $x \in \mathbb{R}^n$ is the state vector, $u \in \mathbb{R}^m$ is the input, $y \in \mathbb{R}^q$ is the output, $v \in \mathbb{R}^p$ is an unknown input, $h \in \mathbb{R}^j$ is the measurement perturbation, and $A \in \mathbb{R}^{n\times n}$, $B \in \mathbb{R}^{n\times m}$, $C \in \mathbb{R}^{q\times n}$, $D_f \in \mathbb{R}^{n\times n}$, $H \in \mathbb{R}^{n\times n}$, $D \in \mathbb{R}^{n\times q}$ and $R \in \mathbb{R}^{q\times j}$ are the system matrices. The nonlinearity $f(Hx)$ is assumed to fulfill the following conditions [8].

Condition 1: The nonlinearity $f(Hx)$ satisfies the OSL condition if the following inequality is valid:

$$\langle f(H\hat{x}) - f(Hx), H(\hat{x} - x)\rangle \leq \rho \|H(\hat{x} - x)\|^2. \tag{2}$$

Defining $\Delta f = f(H\hat{x}) - f(Hx)$ and $e = \hat{x} - x$, Equation (2) can be rewritten as:

$$\Delta f^T He \leq \rho e^T H^T He, \tag{3}$$

where $\rho \in \mathbb{R}$ is the OSL constant.

Condition 2: The nonlinearity $f(Hx)$ satisfies the QIB condition if the following inequality is valid:

$$\|f(H\hat{x}) - f(Hx)\|^2 \leq \beta \|H(\hat{x} - x)\|^2 + \gamma \langle f(H\hat{x}) - f(Hx), H(\hat{x} - x)\rangle. \tag{4}$$

Defining $\Delta f = f(H\hat{x}) - f(Hx)$ and $e = \hat{x} - x$, Equation (4) can be rewritten as:

$$\Delta f^T \Delta f \leq \beta e^T H^T He + \gamma \Delta f^T He, \tag{5}$$

and the scalars γ, β in (5) are the QIB constants.

It should be noted that every vector function that is locally Lipschitz satisfies the one-sided Lipschitz property, but the inverse is not true [8]. For instance, the scalar function $f(x) = -x^3$ is locally Lipschitz but not globally Lipschitz [20]. However, by applying (3) it is possible to conclude that the condition is fulfilled with $\rho = 0$, and thus the system is OSL.

From the above, it can be inferred that the OSL condition encompasses a much larger family of dynamical systems than the classical Lipschitz condition. Hence, the design of an observer with this property could estimate the unknown state of a wide variety of systems (larger than including the classical Lipschitz property). To guarantee an implementable design of the observer, it is of vital importance to guarantee robustness against perturbations in the measurement (usually modeled as noise) since it can negatively alter the performance of the observer. Thus, the goal of this work is to propose a formulation of a state estimator that is robust with respect to noise and which also includes the OSL-QIB property. With these characteristics, the implementation of the observer becomes interesting for real-time state estimation and filtering applications.

In order to present the results obtained in this paper, the following preliminary definitions are necessary:

Definition 2.1. (Exponential Observer) [21]: An observer $\hat{x}$ is an exponential observer of x with convergence rate α and overshoot Ω if the following inequality holds for all $t \geq 0$:

$$\|x(t) - \hat{x}(t)\| \leq \Omega \|x(0) - \hat{x}(0)\| e^{-\alpha t}. \tag{6}$$

Definition 2.2. (Continuous time robust observer)[21]: An observer $\hat{x}$ of x with $\mathcal{L}_2$ gain μ is said to be robust with respect to perturbation v, if :

$$\int_0^\infty (e(s)^T e(s) - \mu^2 v(s)^T v(s)) ds < 0, \tag{7}$$

where $e(s)$ corresponds to the estimation error $(\hat{x}(s) - x(s))$.

3. Unknown Input Observer design for QIB-OSL nonlinear systems

3.1. UIO design, including sensor perturbations ($R \neq 0$)

This section will address the design of a UIO when the measurement is perturbed, that is, $R \neq 0$. Initially, let us consider the following UIO structure [8]:

$$\begin{aligned} \dot{z} &= Nz + TBu + Gy + TD_f f(H\hat{x}), \\ \hat{x} &= z - Ey, \end{aligned} \tag{8}$$

where z is the auxiliary variable, $\hat{x}$ is the estimation of the system state, and matrices N, J, L, E and $T = I_n + EC$ are the observer gains. The subtraction between the estimated state and the real state of the system allows to define the estimation error as

$$\begin{aligned} e &= \hat{x} - x = z - ECx - x = z - Tx, \\ T &= (I_n + EC). \end{aligned} \tag{9}$$

Taking the time derivative of (9), the error dynamics can be deduced. Considering that $R \neq 0$, it is possible to obtain the following error dynamics:

$$\dot{e} = Ne + (GR + NER)h + TD_f \Delta f - ER\dot{h} - TDv(t). \tag{10}$$

From (10) it is easy to observe that the dynamics of the estimation error are influenced by the sensor perturbation and its derivative. Once the error dynamics are obtained, it is possible to proceed with the UIO synthesis [10]. In the following equations, the observer gains are stated as functions of other matrices (that will be used as matrix variables in LME and LMI expressions):

$$\begin{aligned} E &= P^{-1}S, \\ K &= P^{-1}Q, \\ N &= TA - KC, \\ G &= K + KCE - TAE. \end{aligned} \tag{11}$$

In Theorem 1, some conditions are stated in order to reduce the impact of the perturbation which affects the sensor.

Theorem 3.1. *If there exist matrices $P \succ 0$, S, Q and positive scalars τ_1, τ_2, τ_3 and μ such that the following LMIs and LMEs have solution:*

$$\begin{bmatrix} \mathcal{H}(PA + SCA - QC) + a_1 & \Lambda^T & QR \\ \Lambda & -2\tau_2 I_n & 0_n \\ R^T Q^T & 0_n & -\tau_3 \mu^2 I_n \end{bmatrix} \prec 0,$$

$$PD + SCD = 0, \tag{12}$$

$$SR = 0, \tag{13}$$

$$P \succ 0, \tag{14}$$

$$a_1 = 2(\tau_1 \rho + \tau_2 \beta) H^T H + \tau_3 I_n, \tag{15}$$

then observer (8) is a robust observer of system (1) *and its gains are given by (11) , with $\mathcal{L}_2$ gain equal to μ.*

Proof: By assuming $PD + SCD = 0$, and since P is invertible, it follows $D + P^{-1}SCD = 0$, and since $P^{-1}S = E$, $(I + EC)D = 0$, this leads to $TD = 0$.

Furthermore:

$$
\begin{aligned}
NT + GC - TA &= N + NEC + GC - TA \\
&= -KC + NEC + GC \\
&= NEC + (KCE - TAE)C \\
&= (N + KC - TA)EC \\
&= 0.
\end{aligned}
$$

Using the error dynamics (10) and the LME constraint $PD + SCD = 0$, the quadratic Lyapunov function (LF) $V = e^T P e$ is proposed. Taking the LF derivative with respect to time, and adding the LME constraint $SR = 0$ (with the aim to reduce the impact of the sensor perturbation, since $GR = QR$ and $ER = P^{-1}SR = 0$), Equation (16) is obtained:

$$\dot{V} = e^T(N^T P + PN)e + \mathcal{H}(h^T QRe) + \mathcal{H}(\Delta f D_f^T T^T Pe). \tag{16}$$

Pre-multiplying conditions (3) and (5) with the constants $2\tau_1$ and $2\tau_2 \in \mathbb{R}$, respectively, it is possible to find an upper bound for the LF derivative:

$$\Psi = \rho e^T H^T He - \Delta f He > 0, \tag{17}$$

$$\Gamma = \Delta f^T \Delta f + \gamma e^T H^T \Delta f + \beta e^T H^T He > 0, \tag{18}$$

$$\dot{V} \le \dot{V} + \tau_1 \mathcal{H}(\Psi) + \tau_2 \mathcal{H}(\Gamma). \tag{19}$$

Considering Equations (17), (18) and (7), inequality (20) is defined for the LF derivative as follows:

$$\dot{V} \le \dot{V} + \tau_1 \mathcal{H}(\Psi) + \tau_2 \mathcal{H}(\Gamma) + \tau_3 e^T e - \tau_3 \mu^2 h^T h. \tag{20}$$

By introducing the variable $\zeta = [e \quad \Delta f \quad h]$, Equation (20) can be rewritten as an LMI as

$$\zeta^T \begin{bmatrix} \mathcal{H}(PA + SCA - QC) + a_1 & \Lambda^T & QR \\ \Lambda & -2\tau_2 I_n & 0_n \\ R^T Q^T & 0_n & -\tau_3 \mu^2 I_n \end{bmatrix} \zeta \prec 0, \tag{21}$$

$$a_1 = 2(\tau_1 \rho + \tau_2 \beta) H^T H + \tau_3 I_n. \tag{22}$$

Once (21) has been obtained, the proof of Theorem 1 is concluded.

Remark: Notice that it is possible to minimize the impact of the sensor perturbation on the system by replacing $\tau_3 \mu^2$ by a new LMI variable ϵ such that $\frac{\epsilon}{\tau_3}$ is minimized. This minimizes the $\mathcal{L}_2$ gain μ. While $\frac{\epsilon}{\tau_3}$ is not a convex function of the optimization variable, an approximate solution can be found by replacing the cost function by $\epsilon - \tau_3$ such that the resulting optimization problem is convex.

3.2. *UIO design including perturbations in the measurement (alternative approach)*

Upon inspection of Theorem 1, it can be observed that the condition $SR = 0$ might be too restrictive and renders the optimization problem difficult to solve. In order to overcome this problem, Theorem 2 is proposed.

Theorem 3.2. *If there exist matrices $P \succ 0$, S, Q and positive scalars $\tau_1, \tau_2, \tau_3, \tau_4$ and μ such that a solution exists for the following LMIs and LMEs:*

$$\begin{bmatrix} \mathcal{H}(PA + SCA - QC) + a_1 & \Lambda & QR & -SR \\ \Lambda^T & -2\tau_2 I_n & 0_n & 0_n \\ R^T Q^T & 0_n & -\tau_3\mu^2 I_n & 0_n \\ R^T S^T & 0_n & 0_n & -\tau_4\mu^2 I_n \end{bmatrix} \prec 0, \tag{23}$$

$$a_1 = 2(\tau_1\rho + \tau_2\beta)H^T H + \tau_3 I_n, \tag{24}$$

$$PD + SCD = 0, \tag{25}$$

$$P \succ 0, \tag{26}$$

then observer (8) *is a robust observer of* (1) *and its gains are given by (11), with $\mathcal{L}_2$ gain equal to μ.*

Proof: Considering the error dynamics (10), the quadratic LF $V = e^T P e$ is proposed. Taking the LF derivative and adding the LME constraint $PD + SCD = 0$, the following expression is obtained:

$$\dot{V} = \mathcal{H}(e^T PNe) + \mathcal{H}(e^T QRh) - \mathcal{H}(e^T SR\dot{h}) + \mathcal{H}(e^T PTD_f \Delta f). \tag{27}$$

Taking Equations (17) and (18) together with Equation (7) in Definition 2 (proposing $\mathcal{L}_2$ gains for the measurement perturbation and its derivative), inequality (28) is defined for LF derivative as

$$\dot{V} \leq \dot{V} + \tau_1\mathcal{H}(\Psi) + \tau_2\mathcal{H}(\Gamma) + (\tau_3 + \tau_4)e^T e - \tau_3\mu^2 h^T h - \tau_4\mu^2 \dot{h}^T \dot{h}. \tag{28}$$

Introducing the variable $\Xi = \begin{bmatrix} e & \Delta f & h & \dot{h} \end{bmatrix}$, inequality (28) can be rewritten as

$$\Xi \begin{bmatrix} \mathcal{H}(PA + SCA - QC) + a_1 & \Lambda & QR & -SR \\ \Lambda^T & -2\tau_2 I_n & 0_n & 0_n \\ R^T Q^T & 0_n & -\tau_3\mu^2 I_n & 0_n \\ -R^T S^T & 0_n & 0_n & -\tau_4\mu^2 I_n \end{bmatrix} \Xi \prec 0 \tag{29}$$

$$a_1 = 2(\tau_1\rho + \tau_2\beta)H^T H + \tau_3 I_n \tag{30}$$

The effect of the measurement perturbation is minimized in the same way as in Theorem 1. Initially, we propose the change of variables $\epsilon_1 = \tau_3\mu^2, \epsilon_2 = \tau_4\mu^2$, and then solve the semidefinite programming (SDP) $\epsilon_1 - \tau_3 + \epsilon_2 - \tau_4$. This concludes the proof of Theorem 2.

3.3. UIO design, free of sensor perturbations (R=0)

This section will address the design of a UIO when the measurement is perturbation-free, that is, $R = 0$. Initially, considering the UIO structure (8), the expression of the estimation error can be obtained by making the subtraction between the estimated state and the real state:

$$\begin{aligned} e &= \hat{x} - x = z - ECx - x = z - Tx, \\ T &= I_n + EC. \end{aligned} \tag{31}$$

Taking the time derivative of (31), the error dynamics can be deduced:

$$\begin{aligned} \dot{e} &= \dot{z} - T\dot{x}, \\ \dot{e} &= Ne + TD_f\Delta f + (NT + GC - TA)x - TDv. \end{aligned} \tag{32}$$

Theorem 3.3. *If there exist matrices $P \succ 0$, S, Q and positive scalars τ_1, τ_2 such that the following LMIs and LMEs have solution:*

$$\Lambda = D_f^T P + D_f^T C^T S^T - \tau_1 H + \tau_2 \gamma H, \tag{33}$$

$$\begin{bmatrix} \mathcal{H}(PA + SCA - QC) + 2\tau_2\beta H^T H + 2\tau_1\rho H^T H & \Lambda \\ \Lambda^T & -2\tau_2 I_n \end{bmatrix} \prec 0, \tag{34}$$

$$PD + SCD = 0, \tag{35}$$

$$P \succ 0, \tag{36}$$

then observer (8) is an exponential observer of (1)*, and its gains are given by (11), with $\mathcal{L}_2$ gain equal to μ.*

Proof: With the above considerations and the LME constraint $PD + SCD = 0$ analysis, the simplified error dynamics are obtained:

$$\dot{e} = Ne + TD_f\Delta f. \tag{37}$$

Considering the error dynamics (37), the quadratic LF $V = e^T Pe$ is proposed. Taking the LF derivative, the following expression is found:

$$\dot{V} = e^T \left(N^T P + PN\right) e + \mathcal{H}\left(\Delta f \left(D_f^T P + D_f^T C^T S^T\right) e\right). \tag{38}$$

Using (17) and (18), it is possible to find an upper bound for the LF derivative:

$$\dot{V} \leq \dot{V} + \tau_1 \mathcal{H}(\Psi) + \tau_2 \mathcal{H}(\Gamma). \tag{39}$$

Rewriting inequality (39) leads to the following LMI:

$$\Lambda = D_f^T P + D_f^T C^T S^T - \tau_1 H + \tau_2 \gamma H,$$
$$\eta = [e \quad \Delta f],$$
$$\eta^T \begin{bmatrix} \mathcal{H}(PA + SCA - QC) + 2\tau_2 \beta H^T H + 2\tau_1 \rho H^T H & \Lambda^T \\ \Lambda & -2\tau_2 I_n \end{bmatrix} \eta \prec 0. \quad (40)$$

With the determination of LMI (40), the proof of Theorem 3 is finished.
Note that, in the linear case, necessary and sufficient condition were given in [22]. Under those assumptions, and provided the OSL-QIB constant are small enough, then the LMIs in Equation (34) are feasible. This is formally stated in the following proposition:

Proposition 3.4. *Neccessary and sufficient conditions for* (8) *to be a UIO for the system defined by* (1) *are:*

- *$rank(C) = rank(CD)$,*
- *the pair (A_1, C) is detectable, with $A_1 = A - D[(CD)^T CD]^{-1}(CD)^T CA$, and*
- *there exist nonzero OSL-QIB constants such that* (34) *is negative definite.*

Proof. The matrix from the LMI (40) for the case when OSL-QIB constants are 0, can be written defining the variables $\omega = \mathcal{H}(PA + SCA - QC)$, $\mathcal{B} = -2\tau_2 I_n$, $\eta = x = \begin{bmatrix} x_1 & x_2 \end{bmatrix}$ and $\Lambda = D_f^T P + D_f^T C^T S^T - \tau_1 H$. Then, Equation (34) can be rewritten as:

$$x^T \begin{bmatrix} \omega & \Lambda^T \\ \Lambda & \mathcal{B} \end{bmatrix} x = x_1^T \omega x_1 + 2x_1^T \Lambda x_2 + x_2^T \mathcal{B} x_2. \quad (41)$$

From Equation (41), and assuming the detectability condition, it is possible to conclude that:

$$x_1^T \omega x_1 + 2x_1^T \Lambda x_2 + x_2^T \mathcal{B} x_2 \leq -\lambda_{max}(\omega)\|x_1\|^2 + 2\|x_1\|\|x_2\|\|\Lambda\| - \tau_2\|x_2\|^2. \quad (42)$$

Applying Cauchy-Schwarz inequality to the Equation (41), the following relationship is obtained:

$$2\|\Lambda\|\|x_1\|\|x_2\| \leq \frac{\|x_1\|^2\|\Lambda\|}{\varepsilon} + \|x_2\|^2\|\Lambda\|\varepsilon. \quad (43)$$

Using Equations (42) and (43), it is possible to bound the non-definite sign matrix Λ term as follows:

$$x_1^T \omega x_1 + 2x_1^T \Lambda x_2 + x_2^T \mathcal{B} x_2 \leq -(\lambda_{max}(\omega) - \frac{\|\Lambda\|}{\varepsilon})\|x_1\|^2 - (\tau_2 - \|\Lambda\|\varepsilon)\|x_2\|^2, \quad (44)$$

where one can choose ε such that $\lambda_{max}(\omega) - \frac{\|\Lambda\|}{\varepsilon} > 0$.
Then, one can choose τ_2 such that $\tau_2 - \|\Lambda\|\varepsilon > 0$ ensuring

$$\begin{bmatrix} \omega & \Lambda^T \\ \Lambda & \mathcal{B} \end{bmatrix} \prec 0.$$

By continuity of negative definiteness, there exist some small enough OSL-QIB constants such that the (40) is feasible and relationship (42) is fulfilled.

□

3.4. Calculation of the OSL-QIB constants

As a preliminary step to implement the UIO, it is important to determine the OSL and QIB constants. The calculation of these constants can be a complex step for systems with numerous state variables. However, a simple methodology is proposed in [7] to obtain the values of these constants.

To find the OSL constant ρ, matrix $\Psi = \frac{1}{2}\left(J_f + J_f^T\right)$ must be computed, where J_f is the Jacobian of the system. Finding the mathematical expression for Ψ, the optimization problem (45) is solved to find $\rho \in \mathbb{R}$ as

$$\rho = \max_{i \in n}\left(\max_{x,u \in \Omega}\left(\Psi_{i,i} + \sum_{j \in n|i} |\Psi_{i,j}|\right)\right), \tag{45}$$

where Ω is the set of feasible inputs and states.

According to [9], the QIB constants are parameterized in terms of the non-negative variables ϵ_1, ϵ_2 (which add a degree of freedom to the calculation of the QIB constants, which can be very useful when designing observers and controllers). From Equation (5) and [9], the first QIB constant is equal to $\beta = \epsilon_2 - \epsilon_1$, while γ is equal to the solution of the following optimization problem:

$$\gamma = \epsilon_1 \underline{\gamma} - \epsilon_2 \bar{\gamma} + \max_{x,u \in \Omega} \sum_{i \in n} \|\nabla \xi_i\|^2 \geq 0, \tag{46}$$

with

$$\underline{\gamma} = \max_{x,u \in \Omega} \lambda_{max}(\Psi) \tag{47}$$

and

$$\bar{\gamma} = \min_{x,u \in \Omega} \lambda_{min}(\Psi), \tag{48}$$

where λ are the eigenvalues of Ψ and $\|\nabla \xi_i\|^2$ is the norm of each row of J_f. Giving an interpretation of the meaning of the constants, it is possible to say that the QIB constants can be interpreted as a way to "split" the Lipschitz constant, and relax the Lipschitz representation, since QIB constants can be negative [9]. The OSL constant helps in terms of convergence, as it makes the proof of convergence easy to solve, indicating an upper bound of the derivative [9].

4. Application examples

In this section, three application examples are considered for illustrating the proposed approaches: a continuous stirred-tank reactor (CSTR), a water tank-open channel

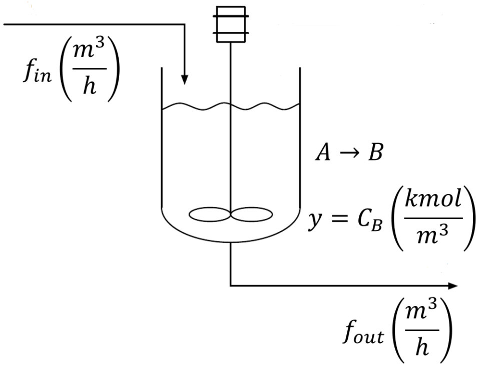

Figure 1. Isothermal CSTR reactor with single reaction [23]

system and the FHN system. The three physical systems are interesting, since in addition to correspond to real processes, the CSTR and the FHN are locally Lipschitz, while the water tank-open channel is OSL in the region of study, which demonstrates the adaptability of the UIO to the different types of nonlinearities that can occur when designing the proposed state estimation scheme. To measure the performance of the UIO in each situation, the Integral Squared Error (ISE), defined as

$$ISE = \int_0^t \| e(t) \|^2 \, dt, \tag{49}$$

is used.

4.1. Isothermal CSTR

CSTR are usually key equipment within the stages of a process, since they are in charge of generating higher value-added products [23]. When operating CSTR, different amounts of reagents are usually added in order to maximize the conversion and the generation of added value products. Thus, it is important to monitor the concentrations of the reagents and products involved at the reaction stage. In order to perform the above task efficiently, the UIO will be used. A schematic representation of the case study to be considered is shown in Figure 1.

Assuming constant level and first order isothermal reaction, the following molar balances are proposed for the chemical species involved in the process [23]:

$$\dot{N}_A = \frac{F_1}{V}(N_{A,in} - N_A) - r_A V, \tag{50}$$

$$\dot{N}_B = -\frac{F_1}{V} N_B + r_A V, \tag{51}$$

$$r_A = k_0 e^{-\frac{Ea}{RT}} \frac{N_A}{V}, \tag{52}$$

Parameter	Units	Value
Reactor volume (V)	m^3	6.6
Preexponential constant (k_0)	h^{-1}	9703.3600
Activation energy (E_a)	$\frac{kcal}{kmol}$	11843
Gas constant (R)	$\frac{kcal}{kmolK}$	1.987
Reactor temperature (T)	$°C$	60
Density (ρ)	$\frac{kg}{m^3}$	1000
Feed concentration of A ($\frac{N_{A,in}}{V}$)	$\frac{kmol}{m^3}$	0.5
Input flow (F_1)	$\frac{m^3}{h}$	5

Table 1. CSTR reactor parameters and inputs

$$x = \begin{bmatrix} N_A & N_B \end{bmatrix}, \quad y = N_B, \quad u = F_1, \tag{53}$$

where N_A and N_B are the moles of reagent and product, respectively, F_1 is the volumetric input flow, and r_A is the velocity of consumption for the reagent. The parameters in Equations (50)–(52) are summarized in Table 1 [23].

From the knowledge of the process dynamics and parameters, the system can be rewritten in the form of (1) with the following matrices:

$$A = \begin{bmatrix} -k_0 e^{-\frac{Ea}{RT}} & 0 \\ k_0 e^{-\frac{Ea}{RT}} & 0 \end{bmatrix}, \quad B = \begin{bmatrix} 0 \\ 0 \end{bmatrix}, \tag{54}$$

$$H = D_f = I_2, \tag{55}$$

$$R = C = \begin{bmatrix} 1 & 0 \end{bmatrix}, \quad D = R^T \tag{56}$$

$$f = \begin{bmatrix} \frac{F_1}{V}(N_{A,in} - N_A) \\ -\frac{F_1}{V} N_B \end{bmatrix}. \tag{57}$$

The OSL-QIB constants $\rho = 0$, $\beta = -1$ and $\gamma = -0.2237$ can be computed using Equations (45) and (46). From the value of the constants, we can interpret that this system can provide an easy convergence for the Lipschitz case, since $\rho = 0$, and $L = \sqrt{|\beta| + \gamma^2}$, see [9]. Solving the conditions of Theorem 2 using YALMIP [24], the values that are found for the scalars and matrices are given in Equation (58) and Table 4.1.

$$P = \begin{bmatrix} 3.33 & 0 \\ 0 & 3.33 \end{bmatrix} \qquad Q = \begin{bmatrix} 1.62 \times 10^6 \\ 1.02 \times 10^8 \end{bmatrix} \qquad S = \begin{bmatrix} 0 \\ -3.33 \end{bmatrix} \tag{58}$$

Initially, the observer is tested with the measurement free of noise and the initial conditions $x(0) = \begin{bmatrix} 0 & 0 \end{bmatrix}$, $z(0) = \begin{bmatrix} 0.6 & 0.6 \end{bmatrix}$. Additionally, after 20 hours of operation, an additional flow of product is added to the system with the objective of accelerating the production, i.e., $Dv = \begin{bmatrix} 0 & 2N_B/V \end{bmatrix}$. This flow can be considered as an unknown input. Figure 2 presents the observer performance in the absence of noise.

Parameter	Value
τ_1	2.13×10^8
τ_2	6.62×10^8
τ_3	3.46×10^8
τ_4	3.46×10^8
μ	1.14

Table 2. Scalars of the solution for Theorem 2, CSTR case

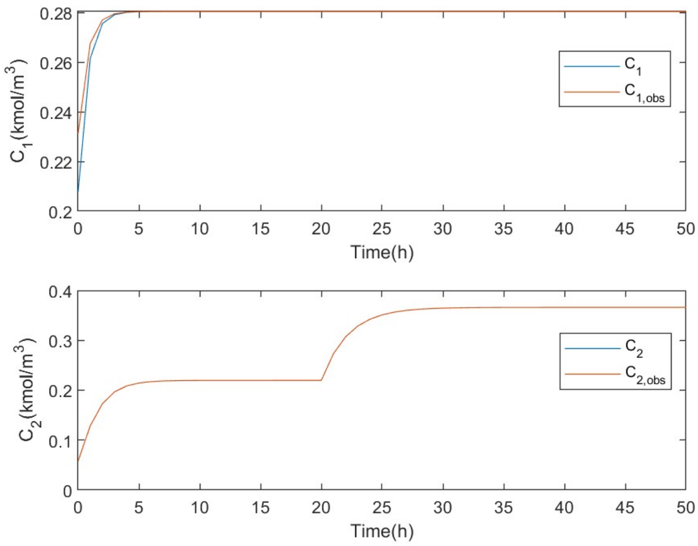

Figure 2. UIO considering Theorem 3, CSTR free of noise case ($ISE = 0.01$)

From the results presented in Figure 2, it can be inferred that the observer converges to the true state in finite time while adapting correctly to the unknown input applied to the reactor. From this figure, it can be seen that the unknown input only affects the product concentration (in order to fulfill the condition $rank(C) = rank(CD)$), hence the reagent concentration remains insensitive to this change. The difference between the observer convergence speeds for each of the states is due to the fact that the non-measurable variable takes longer to replicate than the measurable one.

For the second simulation scenario, the previously established conditions will be retained. However, the measured variable will be contaminated with Gaussian noise (zero mean with a standard deviation equal to 1) to evaluate the properties of the observer in this new situation. Figure 3 shows the results in this case.

Regarding the results obtained for the scenario with measurement perturbation considered as noise, it can be inferred that the observer presents a satisfactory performance since noise filtering is observed, all the while retaining the properties established with Theorem 3, i.e., robustness to unknown input and convergence in finite time.

4.2. Water tank-open channel system

Water is a very important element in most production systems [25], and an efficient way to transport and store it is through an open tank-channel system [26]. The tank

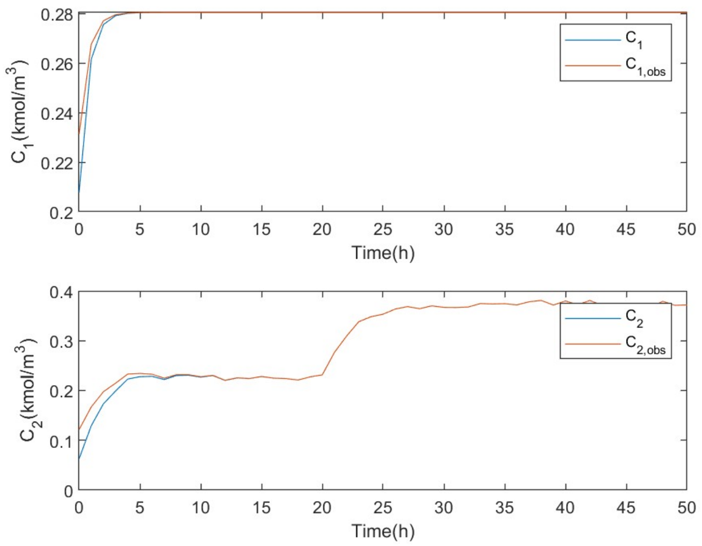

Figure 3. UIO considering Theorem 2, CSTR measurement perturbation case ($ISE = 1.41$)

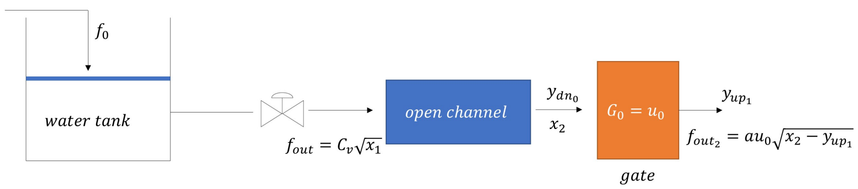

Figure 4. Water tank-open channel system scheme

is in charge of collecting a water flow f_0, which is then supplied through a valve f_{out} to the open channel with a downstream gate f_{out_2} for its subsequent transport and supply. Figure 4 shows the details of the considered case study.

The mathematical model representing the system dynamics is given by the following equations:

$$\dot{h} = f_0 - C_v\sqrt{h}, \tag{59}$$

$$\dot{y}_{dn_0} = C_v\sqrt{h} - au_0\sqrt{y_{dn_0} - y_{up_1}}, \tag{60}$$

$$y = y_{dn_0}, \quad u = f_0, \quad x = \begin{bmatrix} h & y_{dn_0} \end{bmatrix}. \tag{61}$$

Equations (59) and (60) represent the mass balances applied over the system in Figure 4. The term $C_v = 0.1$ is the valve coefficient, $a = 3.98$ is a factor which takes into account the gate properties (geometry and discharge coefficient) and the gravity, $u_0 = 0.4$ is the degree of gate opening, $h = x_1$ is the height of the tank, $x_2 = y_{dn_0}$ is the height before the gate discharge and $y_{up_1} = 0.1$ is the height upstream.

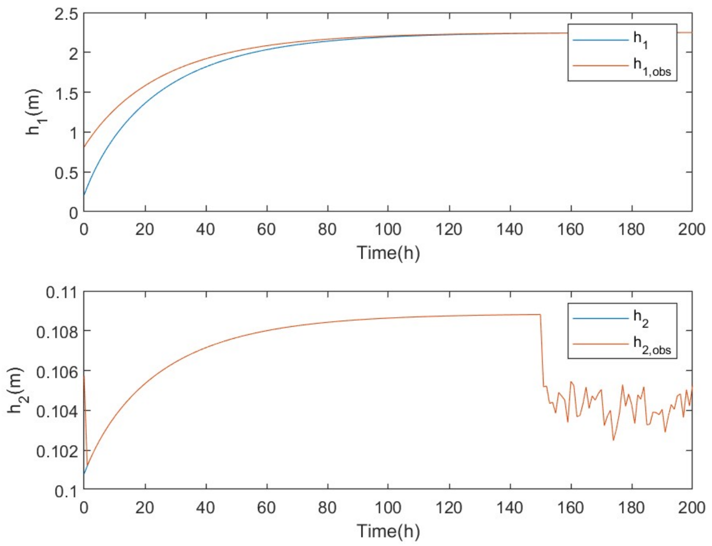

Figure 5. UIO water tank- open channel free of perturbation, Theorem 3 ($ISE = 3.51$)

Rewriting the system in the form of (1), the following matrices are obtained:

$$A = \begin{bmatrix} -0.0333 & 0 \\ 0.0333 & -12.6 \end{bmatrix}, \tag{62}$$

$$H = D_f = I_2, \tag{63}$$

$$R = C = \begin{bmatrix} 0 & 1 \end{bmatrix}, \qquad D = R^T, \tag{64}$$

$$f = \begin{bmatrix} f_0 - C_v\sqrt{h} \\ C_v\sqrt{h} - au_0\sqrt{y_{dn_0} - y_{up_1}} \end{bmatrix} - Ax. \tag{65}$$

In order to implement the observer, the OSL-QIB constants were calculated, obtaining the following values: $\rho = 0, \beta = -0.1, \gamma = -1$ (since γ is unbounded the selected value easily adapts to the OSL condition). The performance of the observer is first evaluated when the measurement is perturbation-free and with initial conditions $x(0) = \begin{bmatrix} 0.1 & 0.1 \end{bmatrix}, z(0) = \begin{bmatrix} 0.6 & 0.6 \end{bmatrix}$. After 160 hours of operation, an unknown input, which can be interpreted as a leak, is applied to the system in order to test the performance of the observer. The results for the simulation of the UIO together with the system under consideration can be found in Figure 5.

The trajectories of the variables in Figure 5 show that the observer is robust to unknown inputs and converges in finite time to the real values of the state variables. Note that the unknown input does not affect the unmeasured variable, since the first dynamic is decoupled of the tank height.

A second simulation case is considered, but this time the measurement is contaminated with Gaussian noise as perturbation (zero mean with standard deviation equal

Parameter	Value
τ_1	1.34
τ_2	11.53
τ_3	1.2
τ_4	1.2
μ	12

Table 3. Scalars of the solution for Theorem 2, Open channel-water tank case

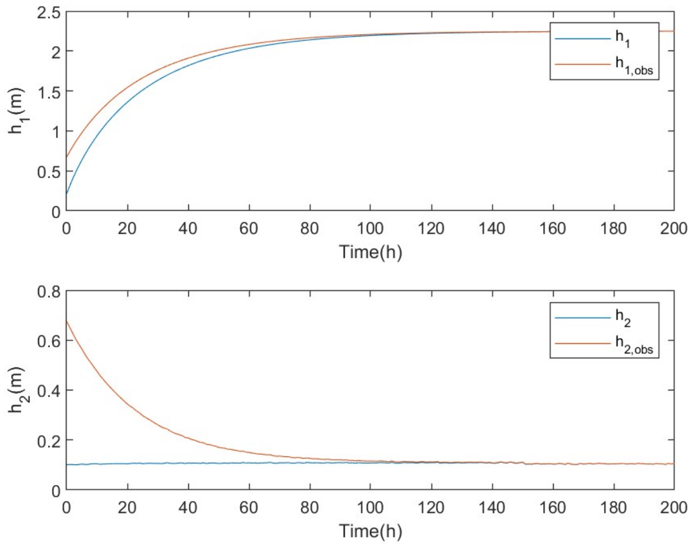

Figure 6. UIO water tank-open channel with noise, Theorem 2 $ISE = 6.03$

to 1), while the rest of conditions are maintained as in the previous case (perturbation-free tank-open channel). The solution of the LMIs stated in Theorem 2 (noisy case) are summarized in the equation (66), and Table 4.2.

$$P = \begin{bmatrix} 7.88 & 0 \\ 0 & 1.06 \end{bmatrix} \qquad Q = \begin{bmatrix} 0 \\ 52.27 \end{bmatrix} \qquad S = \begin{bmatrix} 0 \\ -1.06 \end{bmatrix} \tag{66}$$

Analyzing the results, it can be concluded that the observer retains the robustness against the unknown input in addition to filtering the noise.

4.3. FitzHugh-Nagumo (FHN) system

FHN systems are widely used to model neural behavior, chemical reaction kinetics, artificial neural networks and electronic oscillators, and also to study external stimulation (such as deep brain stimulation) therapies for effective treatment of brain disorders [27]. The following state-space model represents two coupled synchronous

FHN neurons [27]:

$$A = \begin{bmatrix} -g_1-1 & -v_1 & g_1 & 0 & 0 \\ b_1 & 0 & 0 & 0 & 0 \\ g_2 & 0 & -g_2-1 & -v_2 & 0 \\ 0 & 0 & b_2 & 0 & 0 \\ 1 & 0 & -1 & 0 & -1 \end{bmatrix}, \quad C = \begin{bmatrix} 1 \\ 0 \\ 0 \\ 0 \\ 0 \end{bmatrix}^T, \tag{67}$$

$$R = C, \quad D = C^T, \tag{68}$$

$$H = D_f = diag(\begin{bmatrix} 1 & 0 & 1 & 0 & 0 \end{bmatrix}), \tag{69}$$

$$f = \begin{bmatrix} -rx_1^3 + (1+r)x_1^2 + \frac{a}{\omega} cos\omega t \\ 0 \\ -rx_3^3 + (1+r)x_1^3 + \frac{a}{\omega} cos\omega t \\ 0 \\ 0 \end{bmatrix}, \tag{70}$$

$$x = \begin{bmatrix} x_1 \\ x_2 \\ x_3 \\ x_4 \\ x_5 \end{bmatrix}, \quad y = x_1. \tag{71}$$

The parameters are chosen following [27] as $r = 10, a = 1, \omega = 0.26\pi, g_1 = 0.7, g_2 = 1, b_1 = 0.8, b_2 = 1.2, v_1 = b_1^{-1}$ and $v_2 = b_2^{-1}$. Moreover, the OSL-QIB constants take the following values: $\rho = \gamma = 0.1, \beta = 0.2$. In the perturbation-free case, considering the unknown input $v = 0.15sin(10t)$ leads to the results depicted in Figure 7.

Unlike the previous cases, in this situation there is a small bias in the estimation of the states. However, in terms of magnitude it is small (less than 16.16% in average), and it can be concluded that the observer presents a good performance. It should be noted that this system has stronger nonlinearities (square and cubic terms with cosine functions) than the previous case studies, which were bilinear systems, a fact that could make the obtaining of the OSL-QIB constants too accurate. A second simulation case is proposed, considering noise in the measurement as perturbation.

Figure 8 shows that the error dynamics for each of the state variables converges to 0. This is due to the fact that, although the noise and its derivative are minimized during process operation, eliminating its negative effect is very demanding since the condition $SR = 0$ cannot always be fulfilled. However, this proves the fact that the observer could be implemented in complex situations and that its performance is satisfactory when testing various application cases. The solution for the LMIs of Theorem 2 for this

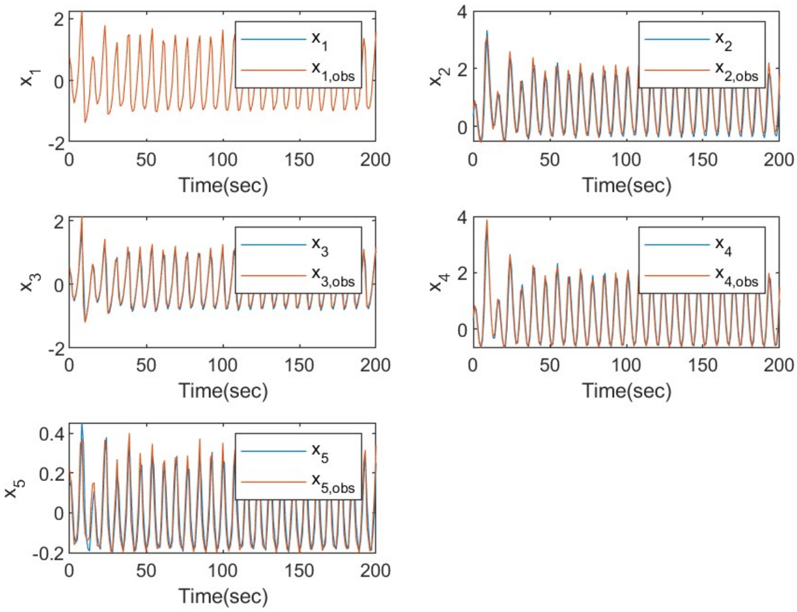

Figure 7. FHN system simulation perturbation-free, Theorem 1 ($ISE = 40.8$)

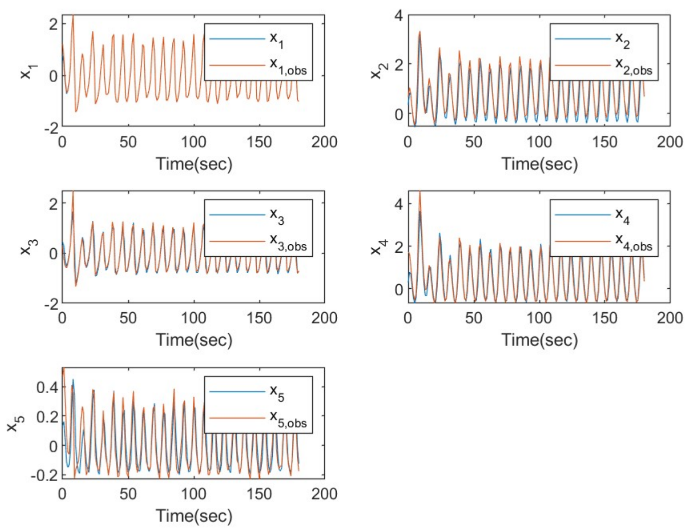

Figure 8. FHN system simulation with noise, Theorem 2 $ISE = 52.6$

example are given in Equation (72) and Table 4.3:

$$P = \begin{bmatrix} 77132764.06 & -2.08 & -3922972.69 & -24080547.76 & -12918864.12 \\ -2.08 & 17.65 & -2.78 & -11.22 & -6.47 \\ -3922972.69 & -2.78 & 104351805.11 & 46884683.21 & -25375909.61 \\ -24080547.76 & -11.22 & 46884683.21 & 133160910.26 & -8695268.95 \\ -12918864.12 & -6.47 & -25375909.61 & -8695268.95 & 100432023.61 \end{bmatrix} \quad (72)$$

Parameter	Value
τ_1	1.43×10^8
τ_2	9.81×10^7
τ_3	0.0064
τ_4	0.0064
μ	1.8×10^5

Table 4. Scalars of the solution for Theorem 2, FHN case

$$Q = \begin{bmatrix} 87749013.71 \\ 1.66 \\ 46293412.61 \\ 22249385.82 \\ 59929672.94 \end{bmatrix} \qquad S = \begin{bmatrix} -77132764.06 \\ 2.08 \\ 3922972.69 \\ 24080547.76 \\ 12918864.12 \end{bmatrix} \tag{73}$$

Remark: The observer for Lipschitz systems proposed by [10] was implemented in the FHN example for comparison purposes. However, the feasibility conditions could not be satisfied just considering the Lipschitz constant. This case exemplifies the advantage of describing a nonlinear system using the OSL-QIB constants, given that the Lipschitz constant does not provide sufficient information in certain cases to obtain satisfactory design conditions for nonlinear observers.

5. Conclusions

This paper presented unknown input observer design strategies for nonlinear OSL-QIB noisy systems that lead to the solution of a set of LMIs/LMEs. Nonlinearities in the state and noise in the measurement were incorporated into the analysis. Based on Lyapunov stability theory, conditions of convergence for the observer were developed and tested in different examples (CTSR, water-tank open channel and FHS system) obtaining good performance in the scenarios considered. From the proposed methodology it was possible to develop an estimation algorithm that was capable of filtering the noise and obtaining finite-time convergence for the error dynamics. The results suggest that the observer could be useful in real applications where unknown or unmodeled inputs and instrumentation uncertainty (noise) are present.

As future research directions, it can be interesting to apply the observer strategy to real case studies, such as water systems and chemical processes, taking into account the sensor resolution [28] and improving observer performance in other situations that can arise in practice such as parameter uncertainty , delays or multiagent systems [29].

References

[1] M. Eull, M. Mohamadian, D. Luedtke, and M. Preindl, "A current observer to reduce the sensor count in three-phase pm synchronous machine drives," *IEEE Transactions on Industry Applications*, vol. 55.5, pp. 4780–4789, 2019.

[2] A. T. Nguyen, J. Pan, T. M. Guerra, and Z. Wang, "Avoiding unmeasured premise variables in designing unknown input observers for takagi–sugeno fuzzy systems.," *IEEE Control Systems Letters*, vol. 5.1, pp. 79–84, 2020.

[3] M. Hou and P. Muller, "Design of observers for linear systems with unknown inputs," *IEEE Transactions on Automatic Control*, vol. 37, no. 6, pp. 871–875, 1992.

[4] S. Hui and S. Żak, "Observer design for systems with unknown inputs," *International Journal of Applied Mathematics and Computer Science*, vol. 15, no. 4, pp. 431–446, 2005.

[5] M. Witczak, J. Korbicz, and V. Puig, "An LMI approach to designing observers and unknown input observers for nonlinear systems," *IFAC Proceedings Volumes*, vol. 39, no. 13, pp. 198–203, 2006. 6th IFAC Symposium on Fault Detection, Supervision and Safety of Technical Processes.

[6] B. Alenezi, M. Zhang, S. Hui, and S. H. Żak, "State observers and unknown input estimators for discrete-time nonlinear systems characterized by incremental multiplier matrices," in *2020 59th IEEE Conference on Decision and Control (CDC)*, pp. 5409–5414, 2020.

[7] S. A. Nugroho, V. Hoang, M. Radosz, S. Wang, and A. F. Taha, "New insights on one-sided lipschitz and quadratically-inner bounded nonlinear dynamic systems," in *2020 American Control Conference (ACC)*, pp. 4558–4563, 2020.

[8] W. Zhang, H. Su, F. Zhu, and G. Azar, "Unknown input observer design for one-sided lipschitz nonlinear systems," *Nonlinear Dynamics*, vol. 79, pp. 1469–1479, 07 2014.

[9] S. A. Nugroho, A. F. Taha, and V. Hoang, "Nonlinear dynamic systems parameterization using interval-based global optimization: Computing lipschitz constants and beyond.," *IEEE Transactions on Automatic Control*, vol. 67, no. 8, pp. 3836–3850, 2021.

[10] W. Chen and M. Saif, "Unknown input observer design for a class of nonlinear systems: an lmi approach," in *Proceedings of the 2006 American Control Conference*, pp. 1–5, 2006.

[11] M. C. Nguyen and H. Trinh, "Unknown input observer design for one-sided lipschitz discrete-time systems subject to time-delay," *Applied Mathematics and Computation*, vol. 286, pp. 57–71, 2016.

[12] A. Jmal, O. Naifar, and N. Derbel, "Unknown input observer design for fractional-order one-sided lipschitz systems," *2017 14th International Multi-Conference on Systems, Signals & Devices (SSD)*, pp. 65–69, 2017.

[13] J. Tian and S. Ma, "Unknown input observer design for one-sided lipschitz nonlinear continuous-time singular markovian jump systems," in *2016 12th World Congress on Intelligent Control and Automation (WCICA)*, pp. 1920–1925, 2016.

[14] E. Lucien and et al., "Robust observer synthesis for bilinear parameter varying system," in *Conference on Decision and Control (CDC)*, no. 61, pp. 1900–1905, 2022.

[15] L. Xiaohang, F. Zhu, and J. Zhang, "State estimation and simultaneous unknown input and measurement noise reconstruction based on adaptive h observer," *IEEE Transactions on Industry Applications*, vol. 14, pp. 647–654, 2016.

[16] N. Cuong, P. N. Pathirana, and H. Trinh, "Robust observer design for uncertain one-sided lipschitz systems with disturbances," *International Journal of Robust and Nonlinear Control*, vol. 28.4, pp. 1366–1380, 2018.

[17] A. Sohaira, M. Rehan, and K.-S. Hong, "Observer-based robust control of one-sided lipschitz nonlinear systems.," *ISA transactions*, vol. 65, pp. 230–240, 2016.

[18] G. Sheng and et al., "Fast actuator and sensor fault estimation based on adaptive unknown input observer.," *ISA transactions*, vol. 129, pp. 305–323, 2022.

[19] A. Zemouche and M. Boutayeb, "On lmi conditions to design observers for lipschitz nonlinear systems," *Automatica*, vol. 49, no. 2, pp. 585–591, 2013.

[20] W. Zhang, H. Su, F. Zhu, and S. P. Bhattacharyya, "Improved exponential observer design for one-sided lipschitz nonlinear systems.," *International Journal of Robust and Nonlinear Control*, vol. 16, no. 18, pp. 3958–3973, 2016.

[21] H. K. Khalil, *Nonlinear Control.* Upper Saddle River, NJ 07458.: Prentice Hall, 2015.

[22] R. J. P. Chen, Jie and H.-Y. Zhang., "Design of unknown input observers and robust fault detection filters.," *International Journal of control*, vol. 63, no. 1, pp. 85–105, 1996.

[23] H. S. Fogler, *Elements of Chemical Reaction Engineering.* 500 S State St, Ann Arbor, MI 48109: Pearson Education, 2016.

[24] J. Lofberg, "Yalmip: A toolbox for modeling and optimization in matlab," *IEEE international conference on robotics and automation*, pp. 284–289, 2004.

[25] G. Conde, N. Quijano, and C. Ocampo-Martinez, “Modeling and control in open-channel irrigation systems: A review,” *Annual Reviews in Control*, vol. 51, pp. 153–171, 2021.

[26] P. Segovia, V. Puig, and E. Duviella, “A Multilayer Control Strategy for the Calais Canal,” *IEEE Transactions on Control Systems Technology*, vol. 32, no. 2, pp. 311–325, 2024.

[27] A. Zulfiqar, M. Rehan, and M. Abid, “Observer design for one-sided lipschitz descriptor systems,” *Applied Mathematical Modelling*, vol. 40, pp. 2301–2311, 2016.

[28] Z. Zhongyi and et al., “Zonotopic non-fragile set-membership fusion estimation for nonlinear systems under sensor resolution effects: Boundedness and monotonicity.,” *Information Fusion*, vol. 105, no. 102232, 2024.

[29] C. Ganghui and J. Wang, “Distributed unknown input observer.,” *IEEE Transactions on Automatic Control*, 2023.